Journal of Ovonic Research Vol. 21, No. 5, September - October 2025, p. 605 - 618

Low-cost potassium hydroxide texturing of monocrystalline silicon: a response surface methodology approach for solar cell application

S. Maqsood [a], A. Younus [b], A. A. Algethami [c], H.T. Ali [c], K. Ali [a,*]
[a] Nano-optoelectronics Research Laboratory, Department of Physics, University of Agriculture Faisalabad, 38040 Faisalabad, Pakistan
[b] Department of Physics Govt College Women University Faisalabad, Pakistan
[c] Department of Mechanical Engineering, College of Engineering, Taif University, Kingdom of Saudi Arabia

Improved light trapping and minimal surface reflectance are needed for higher conversion efficiency of the solar cell. Proposed research work has been focused on reducing the light reflection from the substrate. The fabrication of pyramidal structures on the surface of monocrystalline Si (100) wafers is an effective approach for reducing front-surface reflection losses in traditional silicon solar cells. Alkaline solutions are often used for texturing monocrystalline silicon. Tetramethylammonium hydroxide (TMAH) and potassium hydroxide (KOH) are the predominant etchants utilized in the wet anisotropic etching procedure. One of the two etchants, KOH is an economical option that offers significant etch rate anisotropy between Si (100) and Si (111) planes. Enhancing the etch rate is a significant research challenge for both industrial and academic purposes. This research examines the influence of polyvinyl alcohol (PVA) in 1wt% KOH on the etching properties of Si (100). A systematic parametric analysis was performed by adding several concentrations of PVA (0.1%, 0.3%, and 0.5%) to a 1 wt% KOH solution. Texturing was conducted at 100 °C for 20, 30, and 40 mins. The response surface methodology (RSM) suggests solution concentrations as process factors. Without using an antireflection (ARC) layer, an efficient surface texture with average reflectance of 9.05 % was obtained. The antireflection behavior was additionally correlated to the silicon etch rate. RSM indicated optimal values for PVA concentration and time of 0.1% and 30 mins, respectively. Optimizing the strategy and parameters for texturizing high-efficiency silicon solar cells by response surface methodology may prove beneficial. Reflectance was calculated by the diffuse reflectance spectrophotometer (DRS). The surface morphology of Si (100) wafers was examined using scanning electron microscopy.

(Received July 6, 2025; Accepted September 25, 2025)

Keywords: Potassium hydroxide, Response surface methodology, Optimized surface etching, Silicon solar cells

1. Introduction

The construction of pyramids is a traditional technique for reducing reflectance and enhancing the short circuit current in single-crystalline silicon solar cells [1] A crucial phase in solar cell fabrication is the texturing of the silicon wafer, which significantly reduces light reflection. Surface-textured crystalline silicon wafers are utilized to improve light absorption in silicon solar cells. This extends the path length of the incident light [2]. Texturizing mono- and multi-crystalline silicon wafers eliminates saw damage and alters the surfaces of the as-cut wafers to enhance solar radiation absorption. The efficiency of pyramids formed during texturing has been assessed only by reflectance metrics. This is due to Si materials exhibiting a surface reflectance of around 35% within the visible wavelength spectrum [3].

Mechanical engraving, electrochemical etching and plasma etching are all effective techniques for achieving this objective [4]. Wet anisotropic etching is a widely employed technique for producing microstructures such as cavities, diaphragms and cantilevers in silicon bulk

* Corresponding author: khuram_uaf@yahoo.com
https://doi.org/10.15251/JOR.2025.215.605

micromachining. The conventional method for anisotropic wet chemical etching is esteemed for its cost-effectiveness, ease of use, and lack of physical damage to the substrate. It also generates pure metal ions, which are advantageous for high-performance solar cells [5]. This type of etching is done using alkaline solutions (or wet anisotropic etchants) such as potassium hydroxide (KOH)[6-9] , tetramethylammonium hydroxide (TMAH) [10-13], ammonium hydroxide (NH_4OH) [14-16], ethylenediamine pyrocatechol water (EDP) [17-20], cesium hydroxide (CsOH) [21, 22], hydrazine [23] etc.

Under a variety of settings, the etching properties of these etchants have been investigated in detail. The studies indicate that TMAH and KOH are the most effective etchants for diverse applications, frequently characterized both in the presence and absence of alcohol and surfactants. KOH exhibits less anisotropy between the (100) and (111) planes, cheaper prices, and a faster etch rate compared to TMAH. Previous investigations indicate that Si (100) etch rates peak at 20 wt % KOH [24-26]. Beyond this concentration, the etch rate becomes independent of concentration and decreases as the concentration increases or decreases. Despite its lack of CMOS compatibility due to its dissociation into ions, KOH remains a preferred choice in microfabrication due to its numerous advantages. Notwithstanding progress in wet anisotropic etching and batch production techniques, the comparatively sluggish etch rates in KOH-based systems persistently constrain industrial output. Extended exposure to etchants diminishes the etch rate and may compromise masking layers like SiO_2, adversely affecting the productivity and quality of MEMS and NEM production [27]. Methods including ultrasonication and churning have been explored to enhance etch rates; however, they frequently result in structural damage and demonstrate limited efficacy. Alternative methods utilize additives like as oxidizing agents, redox systems, complexants, metallic impurities, and diverse surfactants to expedite the etching process[28, 29].

Conventional KOH–IPA solutions heated to approximately 80 °C are common for the texturization of monocrystalline silicon wafers, facilitating the creation of random pyramidal structures (~10 µm) while eliminating equivalent silicon depths[30, 31]. This approach has challenges due to IPA instability and the necessity for thorough cleaning after slicing, which constrains process stability and scalability [32]. To resolve these difficulties, high boiling point alcohols, such as polyvinyl alcohol (PVA), have been integrated into KOH-based systems. PVA's advantageous characteristics—such as elevated heat stability, viscosity regulation, and masking ability—facilitate improved anisotropic etching, diminish solvent evaporation, and allow for accurate surface structuring. This method offers a cost-efficient, environmentally sustainable, and scalable solution for the fabrication of next-generation silicon solar cells [33].

Response Surface Methodology (RSM) is a robust statistical and mathematical instrument extensively utilized for experimental design, regression analysis, and intricate process optimization [34]. RSM systematically analyses many factors using factorial designs to identify optimal operating conditions and facilitate accurate prediction and control of process behavior [35]. This method is very successful for attaining efficient, dependable, and scalable optimization in sophisticated engineering systems. RSM provides a cost-effective and eco-friendly approach for enhancing surface texturing operations in silicon solar cell production. It enables the identification of optimal etching parameters, aiding in the advancement of high-performance and scalable solar technology [2].

This work presents a streamlined method utilizing KOH with the addition of PVA to improve anisotropic etching efficacy. Moreover, the study delineates optimized parameters for solution concentration, etching duration, etch rate, and reflectivity metrics. The parameters were methodically established utilizing theoretical insights from RSM, offering a solid basis for optimizing the silicon surface texturing process.

2. Experimental

Surface reflectivity was studied by controlling various parameters on P-type Si (100) wafers. In order to prepare the 1×1 cm silicon substrates for texturing, they were cleaned using the conventional RCA approach to eliminate surface impurities. The cleaning solution comprised $HCl:H_2O_2:H_2O$ in a volumetric ratio of 1:1:6. This solution was heated on a magnetic hot plate with

a thermometer to monitor the temperature. The silicon samples were submerged in the HCl: H2O2:H2O solution for 10 mins and then washed in DI water for 5 mins to eliminate heavy metal contamination. This comprehensive cleaning guaranteed the entire elimination of contaminants from the sample surfaces. The silicon wafers were subsequently submerged in a 2% HF solution for 5 mins at an ambient temperature to eliminate the oxide layer. After that, DI water was used to rinse the samples and remove any remaining HF, thereby preventing contamination from impurities in the chemical solutions. For the etching process, a solution of KOH and PVA was used. PVA, being a powder with a high molecular weight of 72,000, needed to be dissolved in the etching solution beforehand. KOH pellets were mixed with DI water to prepare a 1 wt% KOH solution, to which varying concentrations of PVA (0.1%, 0.3%, and 0.5%) were added. To ensure complete dissolution of PVA, the solution was agitated constantly at 80°C for the first 15 mins and then heated to 100°C for the remaining 15 mins. Maintaining the dissolution temperature above 80°C was crucial, as lower temperatures resulted in incomplete PVA dissolution and undesirable surface textures on the silicon wafers. The silicon samples were etched in the 1% KOH solution with different PVA concentrations for varying time periods, as detailed in Table 1. Samples were extracted at intervals of 10 mins, ranging from 20 to 40 mins of etching time. After etching, the samples were thoroughly rinsed in deionized water. Multiple methods were then used to describe the etched surfaces. We used a scanning electron microscope to examine the surface morphology. The reflectance (%) was measured using diffuse reflectance spectroscopy. The gravimetric approach was employed to determine the etching rate by measuring the samples' weight before and after texturing.

Table 1. Etch rate under different concentrations of KOH and PVA (%) at 100 (ºC).

Sample No.	KOH (%)	PVA (%)	Temperature (°C)	Time (min)	Average Reflectance (%)	Reflectanc at 600nm	Etching Rate (µm/min)
1	1	0.5	100	20	16.97	15.9735	0.043
2	1	0.5	100	30	12	11.4172	0.143
3	1	0.5	100	40	26.68	26.1622	0.268
4	1	0.1	100	20	12.12	11.0761	0.429
5	1	0.1	100	30	9.05	8.7322	0.183
6	1	0.1	100	40	12.67	11.7313	0.143
7	1	0.3	100	20	19.08	18.6097	0.197
8	1	0.3	100	30	11.84	10.8079	0.182
9	1	0.3	100	40	22.02	21.7209	0.214

2.1. Multimodal experimental design for texturing of monocrystalline silicon

The RSM method is a statistical approach for formulating the equations and parameters of a regression model by examining quantitative data from relevant experiments. RSM is a set of mathematical and statistical approaches for modeling and analyzing a variety of situations in which multiple factors impact a desired result [36]. The impact of several factors on etch rate of monocrystalline P- type (100) Silicon wafer from diluted solution using KOH and PVA was investigated using a standard RSM design termed centered composite design. For fitting a second order model, the CCD was frequently employed. Modeling is conceivable with this approach, and it only takes a small number of tests. The empirical nature of the mathematical model obviates the necessity of understanding the exact response mechanism during the modelling phase. There are nc central trials with five repeats, 2n axial trails, and 2n factorial trials that make up the CCD. These layouts consist of nc central places (0,0,0,...,0), 2n axial positions (±α,0, 0, …,0), and 2n factorials, each denoted by ±1 sign [37]. Similarly, the number of runs needed to execute the model grows in direct proportion to the number of parameters n. Using fractional factorial designs with a small number of tests, we may evaluate significant effects and interactions in these cases. 2n factorial designs can't estimate each second-order effect individually. As a result, the CCD was used in this work to estimate the interaction and effect on response variable [38]. Analysis of variance was

employed to predict the statistical measures employing RSM to model and improve the responses and their relevant parameters.

The three key phases in this optimization process are conducting statistically structured experiments, assessing of mathematical model coefficients, and prediction of response according to Equation 1.

$$Y=f(X_1, X_2, X_3, X_4, \ldots, X_n) \quad (1)$$

where X_n represents the controlled variable of action known as factor, and Y represents the optimum response variable. Independent variables are assumed to be controllable and uninterrupted through experimentation having negligible errors. To reveal the specific functional association between response surface and independent variables, an appropriate approximation was required [39]. To reduce the impact of confounding factors, a randomized experimental design was used. Using a second-degree polynomial equation as shown in Equation (2), the main goal of the response was to create an empirical model that would connect the prediction of the reaction to the etch rate as a function of time and PVA concentration (%). $Y=f(X_1, X_2, \ldots, X_n)$

$$Y=b'_0+\sum_{i=1}^{n} b_i X_i+\sum_{i=1}^{n} b_{ii} X_i^2+\sum_{i=1}^{n}\sum_{j>1}^{n} b_{ij} X_i X_j \quad (2)$$

Here the dependent variable or predicted response is denoted by Y, the constant coefficient or intercept constant is shown by b'0, the linear coefficient is b i, the quadratic coefficient is b ii, the interaction coefficients are b ij, and the coded values for PVA (%) and time duration are X ij. CCD necessitates a certain amount of tests in addition to the conventional 2^n factorial, which has its starting point in the middle, $2n$ points positioned axially at a distance from center point to construct quadric values and replicate at center say α where n represents the number of variables [40]. Axial points are elected to ensure rotatability, assuring that model response variability remains consistent at all feasible regions equidistant from the design center [41]. The repetition of tests at the center (0 level) is critical and plays a vital role in providing an independent analysis of experimental errors. For two variables, the optimum number of trials at the center (0 level) is five [42]. As a result, four separate variables were each subjected to a total of four experiments:

$$N = 2^n + 2n + n_c = 4 + 4 + 5 = 13 \quad (3)$$

Upon establishing the requisite ranges for the variables, four separate variables were each subjected to a total of four experiments and ±α for axial points. The model's mean level is represented by the 0 level, which is placed in the model's center. We've chosen a concentration of PVA and time in the array of 0.1-0.5% and 20–40 min [2, 43].

3. Results and discussion

Surface texturing is primarily employed to minimize reflection losses at the front surface of a solar cell; achieving optimal performance requires a holistic approach. Compatibility with subsequent cell fabrication steps and cost-effectiveness are crucial considerations. For example, the texturing process, particularly the dimensions of the features created (e.g., pyramids), must be carefully designed to seamlessly integrate with downstream processes like photolithography. This ensures that the texturing technique does not introduce obstacles that hinder the overall efficiency and manufacturability of the solar cells.

Figure 1 shows SEM images of mono-Si silicon wafers etched using a 1% KOH solution at 100°C for various durations and PVA concentrations. The samples were etched for (a) 20 mins with 0.5% PVA, (b) 30 mins with 0.5% PVA, (c) 40 mins with 0.5% PVA, (d) 20 mins with 0.1% PVA, (e) 30 mins with 0.1% PVA, (f) 40 mins with 0.1% PVA, (g) 20 mins with 0.3% PVA, (h) 30 mins with 0.3% PVA, and (i) 40 mins with 0.3% PVA. Using 0.1% PVA for 30 minutes of etching resulted in the best pyramidal formations, as seen in the SEM photos. Under these circumstances, reflectance measurements were very congruent with RSM's theoretical predictions, as shown in Table 2. The SEM images clearly illustrate the etched surfaces of silicon wafers at different concentrations of

KOH and PVA for 30 mins at 100°C. Among the samples, sample 5, etched with 0.1% PVA for 30 mins, exhibited the most etched surface, indicating the optimal conditions for achieving the desired texture.

Table 2. Variable levels and their experimental range.

Parameters	Factors	Variable level		
		-1	0	+1
PVA (%)	A	0.1	0.3	0.5
Time (min)	B	20	30	40

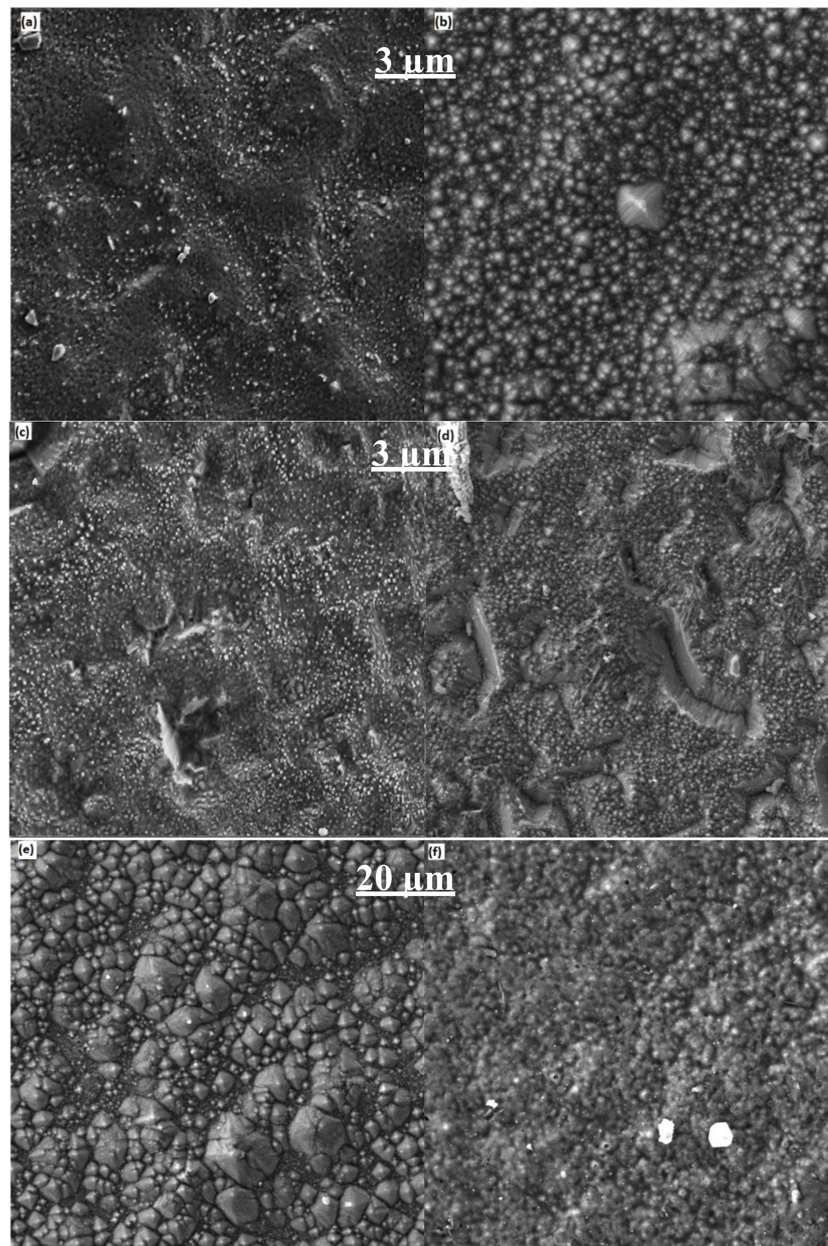

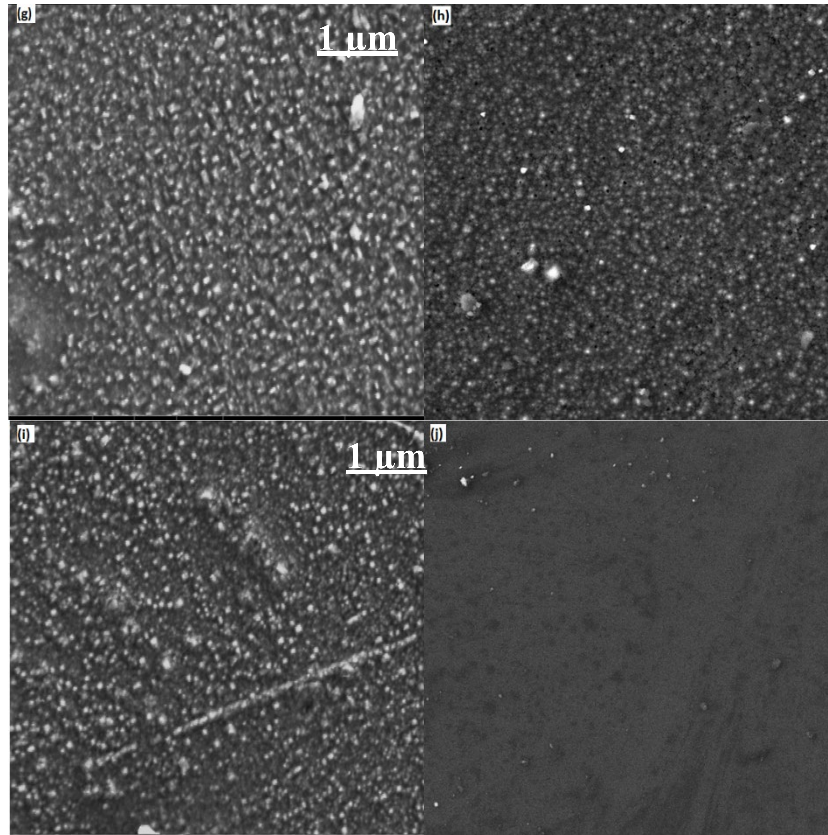

Fig. 1. Top view SEM images (a)S-1,(b) S-2,(c) S-3,(d) S-4,(e) S-5,(f) S-6,(g) S-7,(h) S-8,(i) S-9,(j) as grown Si.

3.1. Statistical analysis

The contour graph of etch rate, reflectance, and standard error of design, along with PVA concentrations and time, indicated the relationship between concentration and its effect on the surface, as shown in Figure 3. From Figure 3 (a), it was evident that with minimal resources, one could determine the desired surface characteristics using RSM and select the appropriate concentrations of PVA and time accordingly. Figure 3 (a) showed that the etch rate decreased with increasing time but remained almost unaffected by increasing concentration. Figure 3 (b) demonstrated that reflectance initially increased with concentration, remained almost constant at 0.1%, and then increased again, reaching 27% reflectance at 0.5% concentration. Figure 3 (c) indicated a standard error of design of 0.889, which was below the statistical limit. The graph suggested that PVA concentration and time ranges of 0.1 – 0.5% and 20 to 40 mins, respectively, had minimal surface effects. The contour graph in Figure 2 (a) illustrated the experiment's desirability, while Figure 2 (b) showed the overlay plot of the etched silicon wafer. Statistical analysis predicted a desirability factor of 1.00 for the experiment. Figure 5 presents plots of reflectivity against wavelength, generated using an optical reflectometer to acquire representative values, and with the sample surfaces considered regarding Lambertian sources. Figure 5 does not include examples 3, 11, 12, and 13 because of the need to prevent duplication, as they had the same PVA concentration of 0.3% and an etching time of 30 mins. Figure 5 demonstrates that the lowest reflectivity obtained in the experiment occurred with a PVA concentration of 0.1% and an etching duration of 30 mins.

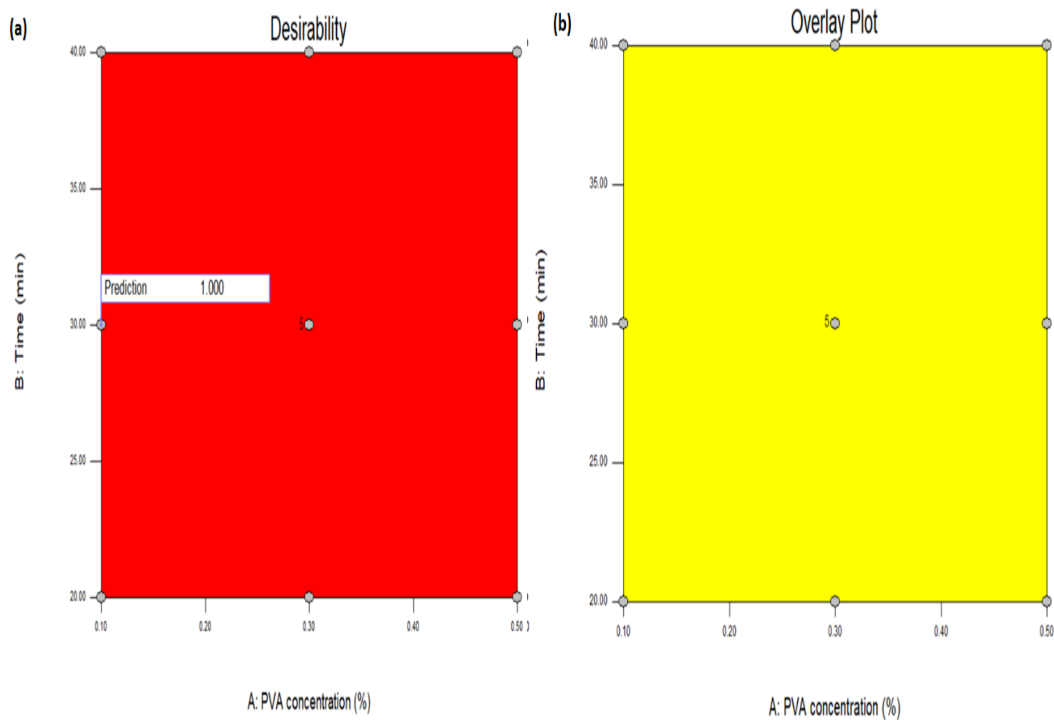

Fig. 2. (a)A graphic showing texturing experiment results on Si wafers at100°C for Disability (b) Overlay plot.

Table 3. Coded level permutation.

Run	Variables		Response	
	A	B	R_1	R_2
1	-1	0	9.05	0.183
2	1	-1	16.97	0.043
3	0	0	12.8	0.253
4	-1	1	12.67	0.143
5	1	1	26.68	0.268
6	0	-1	19.08	0.197
7	0	0	11.84	0.182
8	-1	-1	12.12	0.429
9	0	1	22.02	0.214
10	1	0	12	0.143
11	0	0	12.5	0.185
12	0	0	14.5	0.184
13	0	0	13.2	0.183

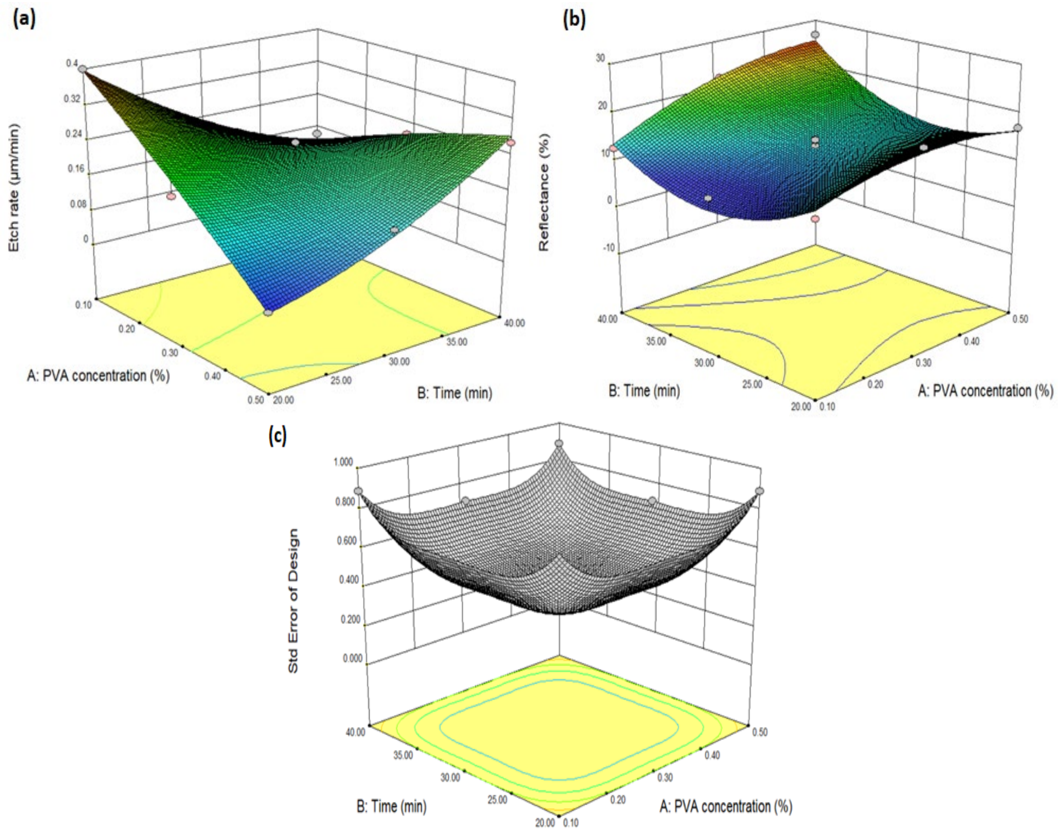

Fig. 3. Combined Effect of PVA and time on (a) Etch rate (µm/min) (b) Reflectance (c) represents standard error of design.

While further trials are need to conclusively validate the findings, Figure 1.4 illustrates the actual and projected reflectivity and etch rate of p-type (100) silicon (Si). Predicted values were derived using approximation functions determined from the model, while actual values were computed using the RSM for specific runs. Table 1.3 shows the different levels of the variables, together with their corresponding components A and B, which stand for the concentrations of PVA (%) and time (min), respectively. After thirteen iterations, the coded values were shown in this table using three different variable setups. Using the response surface technique, two-dimensional plots were created to evaluate the effects of time and PVA concentration on Si reflectance and etch rate. Si etch rate and reflectance were found to be strongly affected by KOH and PVA concentrations, as shown in the ANOVA findings. We used this statistical model to find the variables' significant and non-significant terms (Tables 4 and 5). Insignificant terms were excluded from the formulated mathematical model to enhance its precision and effectiveness.

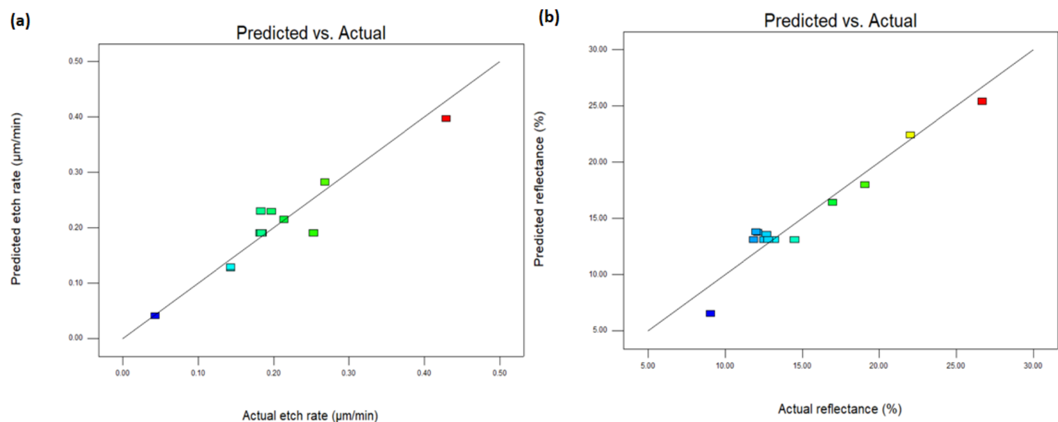

Fig. 4. (a) The actual and predicted plot of Etch rate (µm/min) of silicon (b) Reflectance (%).

The projected values were obtained from the model using approximation functions, whereas the actual values were estimated using response surface data for specific runs. In Table 1.2, you can see the different levels of the variables. Component A stands for the percentage of PVA concentration, and component B for the duration of time in minutes. Table 1.3 displays the coded numbers representing the outcomes for all thirteen runs with the three distinct designs. In Tables 1.4 and 1.5, you may find the non-significant terms, most likely caused moderate correlation coefficients. This was likely caused by a combination of factors, including the large variety of variables used, the small sample size, and the nonlinear relationship between the process response and the examined parameters.

3.2. Establishment of regression model equation

In order to determine the relationship between the etch rate, reflectivity, time, and PVA concentration of a Si p (100) wafer, a face-centered composite design was used. By the halfway point of the thirteen trials, the experimental error had been measured. According to the sequential model sum of squares, the models were chosen using the F value. The independent variables of the model were significant, ensuring that the models were not aliased, and the quadratic model was adopted as proposed by the software [44]. The experiments were tailored to include 13 trials with a star configuration (0, ±1) and their repeats in the center, as per the quadratic model. You can find all the information about the experiment and its results in Table 1.6. The lowest reflectivity was found to be 9.05% and the related etch rate to be 0.183 µm/min. The relationship between etch rate and silicon wafer reflectivity was represented using a regression model. Equation (1.1) provides a mathematical framework that shows the reflectivity (Y) as a function of concentration (X_1) and time (X_2), where the variables represent their coded values. Equation (1.4) shows the final empirical model for coded factors of the silicon wafer's reflectivity and etch rate (Y).

Table 4. ANOVA for fitted model.

Source	Sum of Squares	DF	Mean Square	F Value	Prob > F
For Reflectance					
Model	268.71	5	53.74	18.62	0.0006*
Residual	20.2	7	2.89		
Lack of Fit	16.28	3	5.43	5.54	0.0659
Pure Error	3.92	4	0.98		
Cor Total	288.91	12			
CV	11.30				
For Etch rate $R^2 = 0.9023$					
Model	0.083554	5	0.016711	12.92	0.0020
Residual	0.009051	7	0.001293		
Lack of Fit	0.005182	3	0.001727	1.79	0.2890
Pure Error	0.003869	4	0.000967		
Cor Total	0.092605	12			
CV	17.93				

*Significant at "Prob >F" less than 0.05.

Table 5. Using the least fit and estimating the parameters.

Model Term	**Coeffcient estimate**	**Standard error**	**F -Value**	**Prob > F**
For Reflectance				
Intercept	13.11	0.71	18.62	0.0006*
A-PVA concentration	3.64	0.69	27.47	0.0012
B-Time	2.20	0.69	10.06	0.0157
AB	2.29	0.85	7.27	0.0308
A^2	-2.92	1.02	8.18	0.0243
B^2	7.10	1.02	48.25	0.0002*
R^2 = 0.9301				
Adj R^2= 0.8801				
For Etch rate				
Intercept	0.19	0.015	12.92	0.0020*
A-PVA concentration	-0.050	0.015	11.68	0.0112
B-Time	-7.333E-003	0.015	0.25	0.6327
AB	0.13	0.018	50.48	0.0002
A^2	-0.010	0.022	0.23	0.6445
B^2	0.032	0.022	2.20	0.1819
R^2 = 0.9023				
Adj R^2=0.8324				

*Significant at "Prob >F" less than 0.05.

The reasonable correlation coefficient observed in Table 4 may be influenced by the presence of insignificant terms. This is probably because to the extensive array of diverse variables examined with a restricted number of trials, additionally to the non-linear effects of the variables on the reaction of the process. According to Table 4, the whole model has a considerable statistical value. Model terms are considered important when the value of "Prob > F" is less than 0.0500, whilst values beyond 0.1000 imply that the model components lack significance. The "Model F-Value" of 18.62 for reflectance and 12.92 for etch rate indicate the model's relevance, with hardly a 0.01% likelihood that such substantial "Model F-Values" could arise from noise.

Table 6. Protocol for an experiment to determine the expected and observed outcome.

Run	Variables		Responses					
	A	B	R_1 (Reflectance)			R_2(Etch rate)		
			Actual	Predicted	Residuals	Actual	Predicted	Residuals
1	-1	0	9.05	6.55	2.50	0.18	0.23	-0.047
2	1	-1	16.97	16.43	0.54	0.043	0.042	0.001394
3	0	0	12.8	13.11	-0.31	0.25	0.19	0.062
4	-1	1	12.67	13.56	-0.89	0.14	0.13	0.016
5	1	1	26.68	25.41	1.27	0.27	0.28	-0.014
6	0	-1	19.08	18.01	1.07	0.20	0.23	-0.033
7	0	0	11.84	13.11	-1.27	0.18	0.19	-0.00855
8	-1	-1	12.12	13.74	-1.62	0.43	0.40	0.032
9	0	1	22.02	22.41	-0.39	0.21	0.22	-0.00129
10	1	0	12	13.82	-1.82	0.14	0.13	0.013
11	0	0	12.5	13.11	-0.61	0.19	0.19	-0.00555
12	0	0	14.5	13.11	1.39	0.18	0.19	-0.00655
13	0	0	13.2	13.11	0.094	0.18	0.19	-0.00755

This study aimed to identify optimal parameters within the established mathematical model equations to minimize light reflection. The two-factor model equation was refined within the experimental parameters, and the two-factor interaction yielded significant outcomes. As shown in Table 7, for P-type silicon, the optimal etch rate was achieved with a combination of 0.1% PVA concentration and a 30-mins processing time.

Table 7. Optimized etch rate and reflectance at optimal conc (%) and duration (mins).

	Parameter		Response		Desirability
	A	B	R_1	R_2	
Optimized value	0.1	30	0.23	6.55	1.00

$$\text{Etch rate} = +0.19 - 0.050\,A - 7.333E\text{-}003B + 0.13\,AB - 0.010\,A^2 + 0.032\,B^2$$

$$\text{Reflectance} = +13.11 + 3.64\,A + 2.20\,B + 2.29\,AB - 2.92\,A^2 + 7.10\,B^2 \quad (4)$$

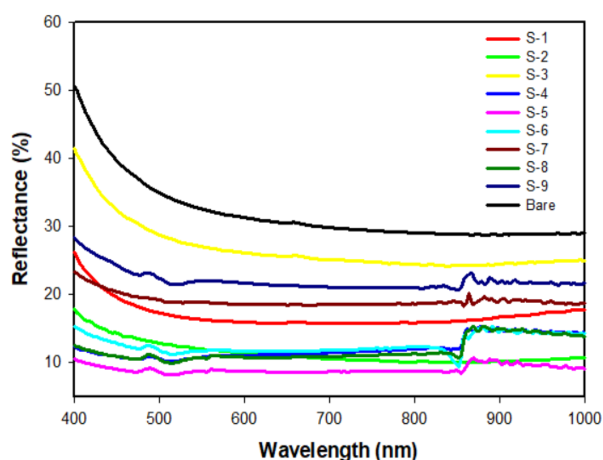

Fig. 5. Reflectance curve as function of wavelength of all samples.

Our etching process effectively reduced the reflectance of the silicon wafer, achieving a minimum value of approximately 9% as illustrated in Figure 5. Diffuse reflectance spectroscopy was employed to quantify reflectance across all nine etched samples and the unprocessed reference silicon wafer. As evident from the figure, the reflectance of the unprocessed silicon reaches nearly 35% within the visible light spectrum. The data reveals that minimum reflectance, and consequently, maximum light trapping, occurs in the 500-800 nm range. Notably, all treated samples exhibit a significant decrease in reflectance compared to the reference. At roughly 600 nm, S-5 exhibits minimal reflectance (around 8%), indicating that optimal light absorption transpires near this wavelength. This is logical as 600 nm represents the apex of the solar spectrum (AM1.5), prompting materials to be frequently optimized for efficient light absorption at this wavelength. The average reflectance for the untreated silicon wafer was 35.2%, while sample 5 demonstrated a remarkably lower average reflectance of 9.05%. All samples showed a reduction in light reflection, with the R_{av} values calculated from diffuse reflectance spectroscopy (DRS) presented in Table 1. For all samples the reflectance value at 600 nm is also provided in Table 1. Table 1 displays the samples' reflectance at 600 nm.

4. Conclusion

An effective framework for optimizing the effect of etching time (20-40 min) and PVA concentration (0.1-0.3%) on the reflectivity of monocrystalline Si (100) wafers was developed by integrating response surface methodology with a face-centered composite design. Design Expert

Software was used to anticipate responses across all experimental regions via the use of response surfaces, statistical significance, and regression analysis. These models successfully connected the process variables with critical responses, facilitating precise predictions throughout the experimental area. Analysis of the response surfaces indicated that although etching duration affects reflectivity reduction, PVA concentration is the primary factor determining surface shape and optical performance. The optimization of processes through the developed models demonstrated exceptional concordance between experimental and projected outcomes, validating the efficacy of the method. The experimentally attained minimum reflectivity was 9.05%, closely aligning with the model-predicted minimum of 6.55%, at an optimized etch rate of 0.23 µm/min. The ideal parameters 0.1% PVA concentration and 30-mins etching duration undertake the efficacy of PVA-assisted KOH etching in generating homogenous, low-reflectivity surfaces. While further experimental trials need to be conducted to enhance the validity of our findings, specific process factors have been identified that yield photovoltaic device manufacturing processes are compatible with these materials, and they consistently exhibit low reflectance.

Acknowledgment

The authors acknowledge the support from the Higher Education Commission (HEC) of Pakistan [Grant No: 8615/Punjab/NRPU/R&D/HEC/2017] for this work. The authors also extend their appreciation to Taif University, Saudi Arabia, for supporting this work through project number TU-DSPP-2024-285.

Funding

This research was funded by Taif University, Taif, Saudi Arabia, Project No. (TU-DSPP- 2024-285).

References

[1] Iencinella, D., et al., An optimized texturing process for silicon solar cell substrates using TMAH. 2005. 87(1-4): p. 725-732; https://doi.org/10.1016/j.solmat.2004.09.020

[2] Ali, K., et al., Low-cost anisotropic etching of monocrystalline Si (1 0 0): Optimization using response surface methodology. 2012. 52(4): p. 782-792; https://doi.org/10.1016/j.spmi.2012.06.008

[3] Kwon, S., et al., Effects of textured morphology on the short circuit current of single crystalline silicon solar cells: evaluation of alkaline wet-texture processes. 2009. 9(6): p. 1310-1314; https://doi.org/10.1016/j.cap.2008.12.014

[4] Lv, H., et al., Porous-pyramids structured silicon surface with low reflectance over a broad band by electrochemical etching. 2012. 258(14): p. 5451-5454; https://doi.org/10.1016/j.apsusc.2012.02.033

[5] Basu, P.K., A. Khanna, and Z.J.R.e. Hameiri, The effect of front pyramid heights on the efficiency of homogeneously textured inline-diffused screen-printed monocrystalline silicon wafer solar cells. 2015. 78: p. 590-598; https://doi.org/10.1016/j.renene.2015.01.058

[6] Rola, K.P., I.J.M.t. Zubel, Impact of alcohol additives concentration on etch rate and surface morphology of (100) and (110) Si substrates etched in KOH solutions. 2013. 19: p. 635-643; https://doi.org/10.1007/s00542-012-1675-x

[7] Rao, A.V.N., et al., Effect of NH2OH on etching characteristics of Si {100} in KOH solution. 2017. 6(9): p. P609; https://doi.org/10.1149/2.0161709jss

[8] Dutta, S., et al., Fabrication of comb structure with vertical sidewalls in Si (110) substrate by wet etching in boiling KOH solution. 2019. 25: p. 3091-3096; https://doi.org/10.1007/s00542-018-4195-5

[9] Gupta, A., P. Pal, and C.S. Sharma. A facile way of surface texturing of Si {100} using KOH for silicon solar cells. in 2021 Symposium on Design, Test, Integration & Packaging of MEMS and MOEMS (DTIP). 2021. IEEE; https://doi.org/10.1109/DTIP54218.2021.9568684

[10] Papet, P., et al., Pyramidal texturing of silicon solar cell with TMAH chemical anisotropic etching. 2006. 90(15): p. 2319-2328; https://doi.org/10.1016/j.solmat.2006.03.005

[11] Gupta, A., et al., Surface texturing of Silicon {100} in an extremely low concentration TMAH for minimized reflectivity. 2019. 8(10): p. P622; https://doi.org/10.1149/2.0301910jss

[12] Ashok, A., P.J.M.T. Pal, Silicon micromachining in 25 wt% TMAH without and with surfactant concentrations ranging from ppb to ppm. 2017. 23: p. 47-54; https://doi.org/10.1007/s00542-015-2699-9

[13] Wang, L., et al., Improving efficiency of silicon heterojunction solar cells by surface texturing of silicon wafers using tetramethylammonium hydroxide. 2014. 268: p. 619-624; https://doi.org/10.1016/j.jpowsour.2014.06.088

[14] Silva, A., et al., The surface texturing of monocrystalline silicon with NH4OH and ion implantation for applications in solar cells compatible with CMOS technology. 2014. 44: p. 132-137; https://doi.org/10.1016/j.egypro.2013.12.019

[15] Sridharan, S., N. Bhat, K.J.A.P.L. Bhat, Silicon surface texturing with a combination of potassium hydroxide and tetra-methyl ammonium hydroxide etching. 2013. 102(2); https://doi.org/10.1063/1.4776733

[16] Alvarez, H.S., et al., NH 4 OH-B silicon texturing of periodic V-groove channels, upright, and inverted pyramids structures. 2021. 11(3): p. 570-574; https://doi.org/10.1109/JPHOTOV.2021.3059421

[17] Bhat, K.N., et al. Optimization of EDP solutions for feature-size-independent silicon etching. in Micromachining and Microfabrication Process Technology VII. 2001. SPIE; https://doi.org/10.1117/12.442978

[18] Yellampalli, C., et al. Micromachining and Microfabrication Process Technology VIII. 2003. SPIE; https://doi.org/10.1117/12.478257

[19] Dutta, S., et al., Comparison of etch characteristics of KOH, TMAH and EDP for bulk micromachining of silicon (110). 2011. 17: p. 1621-1628; https://doi.org/10.1007/s00542-011-1351-6

[20] Bándy, E., M. Rencz, in 2014 14th Biennial Baltic Electronic Conference (BEC). 2014. IEEE; https://doi.org/10.1109/BEC.2014.7320548

[21] Ju, C., P.J.J.S. Hesketh, A.A. Physical, Measurements of the anisotropic etching of a single-crystal silicon sphere in aqueous cesium hydroxide. 1992. 33(3): p. 191-196; https://doi.org/10.1016/0924-4247(92)80166-Z

[22] Hasan, M.M., F. Rahman, International Manufacturing Science and Engineering Conference. 2024. American Society of Mechanical Engineers; https://doi.org/10.1115/MSEC2024-131691

[23] Declercq, M.J., L. Gerzberg, J.D.J.J.o.T.E.S. Meindl, Optimization of the Hydrazine-Water Solution for Anisotropic Etching of Silicon in Integrated Circuit Technology. 1975. 122(4): p. 545; https://doi.org/10.1149/1.2134257

[24] Shikida, M., et al., Differences in anisotropic etching properties of KOH and TMAH solutions. 2000. 80(2): p. 179-188; https://doi.org/10.1016/S0924-4247(99)00264-2

[25] Sai, H., H. Jia, M.J.J.o.A.P. Kondo, Impact of front and rear texture of thin-film microcrystalline silicon solar cells on their light trapping properties. 2010. 108(4); https://doi.org/10.1063/1.3467968

[26] Hajjiah, A.T., S.K. Zachariah, M.Y.J.J.o.E.R. Ghannam, Study of surface morphology and optical characterization of crystalline and multi-crystalline silicon surface textured in highly

diluted alkaline solutions. 2014. 2: p. 1-16; https://doi.org/10.7603/s40632-014-0009-9

[27] Dziuban, J.A., R.J.S.m. Walczak, Etching microwave silicon [EMSi]-microwave enhanced fast deep anisotropic etching of silicon for micro-electromechanical systems [MEMS]. 2001. 13(1): p. 41-55.

[28] Dziuban, J.A.J.S., A.A. Physical, Microwave enhanced fast anisotropic etching of monocrystalline silicon, 2000. 85(1-3): p. 133-138; https://doi.org/10.1016/S0924-4247(00)00373-3

[29] Chen, J., et al., Study of anisotropic etching of (1 0 0) Si with ultrasonic agitation. 2002. 96(2-3): p. 152-156; https://doi.org/10.1016/S0924-4247(01)00786-5

[30] Aoyama, T., et al., Fabrication of single-crystalline silicon solar cells using wafers sliced by a diamond wire saw. Proc. 25th Europ. PVSEC, 2009. 2429.

[31] Hashmi, G., et al., Texturization of as-cut p-type monocrystalline silicon wafer using different wet chemical solutions. 2018. 124: p. 1-11; https://doi.org/10.1007/s00339-018-1818-8

[32] Chang, T.-H., et al., Efficiency enhancement in GaAs solar cells using self-assembled microspheres. Optics express, 2009. 17(8): p. 6519-6524; https://doi.org/10.1364/OE.17.006519

[33] Ximello Quiebras, J.N., Wet chemical textures for crystalline silicon solar cells. 2013.

[34] Bezerra, M.A., et al., Response surface methodology (RSM) as a tool for optimization in analytical chemistry. Talanta, 2008. 76(5): p. 965-977; https://doi.org/10.1016/j.talanta.2008.05.019

[35] Hanrahan, G. K. Lu, Critical Reviews in Analytical Chemistry, 2006. 36(3-4): p. 141-151; https://doi.org/10.1080/10408340600969478

[36] Dc, M., Design and analysis of experiments. 2001, New York: John Wiley and Sons.

[37] Myers, R., R.S. Methodology, Allyn and Bacon. Response Surface Methodology, New York, 1971.

[38] Sahu, J.N., B.C. Meikap, A.V. Patwardhan, CLEAN-Soil, Air, Water, 2010. 38(5-6): p. 533-542; https://doi.org/10.1002/clen.201000028

[39] Gunaraj, V., N. Murugan, Journal of materials processing technology, 1999. 88(1-3): p. 266-275; https://doi.org/10.1016/S0924-0136(98)00405-1

[40] Sahu, J., J. Acharya, B. Meikap, Journal of Hazardous Materials, 2009. 172(2-3): p. 818-825; https://doi.org/10.1016/j.jhazmat.2009.07.075

[41] Box, G.E., J.S. Hunter, The Annals of Mathematical Statistics, 1957: p. 195-241; https://doi.org/10.1214/aoms/1177707047

[42] Box, G.E., J.S. Hunter, Technometrics, 1961. 3(3): p. 311-351; https://doi.org/10.2307/1266725

[43] Bhattacharya, S., 2021, IntechOpen; https://doi.org/10.5772/intechopen.95835

[44] Arunkumar, N., et al., The International Journal of Advanced Manufacturing Technology, 2012. 63: p. 1065-1072; https://doi.org/10.1007/s00170-012-3970-1